Published in final edited form as:
Dev Biol. 2013 April 1; 376(1): 31–42. doi:10.1016/j.ydbio.2013.01.017.

Regulation of G-protein signaling via Gnas is required to regulate proximal tubular growth in the *Xenopus* pronephros

Bo Zhang[a,b], **Daniel Romaker**[a], **Nicholas Ferrell**[c], and **Oliver Wessely**[a,*]

[a]Cleveland Clinic Foundation, Lerner Research Institute, Department of Cellular and Molecular Medicine, 9500 Euclid Avenue/NC10, Cleveland, OH 44195, USA

[b]LSU Health Sciences Center, Department of Cell Biology and Anatomy, 1901 Perdido Street, New Orleans, LA 70112, USA

[c]Cleveland Clinic Foundation, Lerner Research Institute, Department of Biomedical Engineering, 9500 Euclid Avenue/ND20, Cleveland, OH 44195, USA

Abstract

In the kidney, proximal tubules are very important for the reabsorption of water, ions and organic solutes from the primary urine. They are composed of highly specialized epithelial cells that are characterized by an elaborate apical brush border to increase transport efficiency. Using the pronephric kidney of *Xenopus laevis* we discovered that the G-protein modulator cholera toxin resulted in a dramatic reduction of the proximal tubular size. This phenotype was accompanied by changes in the cytoarchitecture characterized by ectopic expression of the distal tubular marker 4A6 and an impairment of yolk platelet degradation. In addition, cholera toxin caused edema formation. However, this phenotype was not due to kidney defects, but rather due to impaired vasculature development. Based on experiments with antisense morpholino oligomers as well as pharmacological agonists and antagonists, we could show that the complex phenotype of cholera toxin in the pronephric kidney was caused by the hyperactivation of a single G-protein alpha subunit, Gnas. This—in turn—caused elevated cAMP levels, triggered a Rapgef4-dependent signaling cassette and perturbed exo- and endocytosis. This perturbation of the secretory pathway by Ctx was not only observed in *Xenopus* embryos. Also, in a human proximal tubular cell line, cholera toxin or a Rapgef4-specific agonist increased uptake and decreased secretion of FITC-labeled Albumin. Based on these data we propose that the Gnas/cAMP/Rapgef4 pathway regulates the signals inducing the proliferation of proximal tubules to acquire their final organ size.

Keywords

Cholera toxin; Endocytosis; Exocytosis; Pronephric kidney; *Xenopus*; Yolk degradation

Introduction

The kidney is the primary organ for fluid homeostasis (Smith, 1953; Saxén, 1987; Vize et al., 2003b). It is required for waste secretion, but also restricts the loss of water, salts and organic compounds. The functional unit of the kidney, the nephron, is subdivided into individual segments along its proximal–distal axis, each consisting of distinct cell types performing dedicated functions. Proximal tubules, in particular, play a critical role in restricting the loss of biologically important molecules by active re-absorption. To

*Corresponding author: Fax: +1 216 444 9404. wesselo@ccf.org (O. Wessely).

efficiently recover most of the solutes, they not only express high levels of transporters/channels, but also develop an apical brush border, which increases the cell surface exposed to the primary urine. Surprisingly, the molecular mechanisms underlying the functional specification of proximal tubular cells are still poorly understood.

G-protein coupled receptors (GPCRs) are a very large protein family characterized by a seven transmembrane domain. This family consists of over 800 members and regulates many different cellular aspects (Katritch et al., 2012). GPCRs have important roles in homeostasis and neurotransmission. It has also become increasingly clear that they play equally important roles in development such as the regulation of morphogenetic movements in the embryo (Heisenberg and Solnica-Krezel, 2008). In contrast to the diversity of ligands and receptors, intracellular GPCR signaling is relatively simple. In its inactive state a trimeric G-protein complex (consisting of one alpha subunit associated with GDP and a beta/gamma dimer) is bound to the GPCR. Upon receptor activation GDP is replaced by GTP, which causes the dissociation of the alpha subunit from the beta/gamma dimer and the activation of downstream signaling. Different downstream effectors are activated based on the G-protein alpha subunit subtype. For example, the $G\alpha_s$ family increases the cellular cyclic AMP (cAMP) levels, whereas the $G\alpha_i$ family decreases them. The dissociated beta/gamma subunit initiates its own signaling pathway mostly by activating phospholipase C (PLC). To inactivate signaling the GTP bound to the alpha subunit will be hydrolyzed by GTPase activating proteins (GAPs) causing the re-association of the trimeric complex.

Bacterial toxins have been instrumental in functional analyses of GPCRs (Aktories, 2011). Pertussis toxin (Ptx), *Pasteurella multocida* toxin (Pmt) and Cholera toxin (Ctx) interact and modify a specific subset of G-protein alpha subunits and cause their constitutive activation or inhibition. Ptx ribosylates members of the $G\alpha_i$ and $G\alpha_t$ families and thereby prevents dissociation of the trimeric complex resulting in a constitutive deactivation of these G-proteins. Pmt deamidates all the members of the $G\alpha_q$ and $G\alpha_i$ family as well as Gna13 of the $G\alpha_{12/13}$ family at a specific glutamine residue. This prevents their association with GAPs and the hydrolysis of GTP resulting in hyperactivation. Ctx ribosylates the two members of the $G\alpha_s$ family, Gnas and Gnal, preventing GTP hydrolysis. This causes elevated cAMP levels, activation of protein kinase A (PKA) and subsequent phosphorylation of transcription factors such as the cAMP responsive element binding protein CREB. In addition, cAMP triggers signaling via Rapgef3/4 (previously known as Epac1/2), which in turn regulates multiple cellular processes such as exocytosis, cell adhesion and proliferation (Borland et al., 2009).

In this study we utilized the broad range activity of these toxins to explore the possible functions of G-protein signaling during kidney development. While the metanephric kidney present in most of the higher vertebrates is generally used as a model to understand these processes, we here used the *Xenopus* pronephros as a paradigm. Compared to the millions of nephrons in the metanephros, the evolutionarily simpler pronephros has only one bilateral nephron pair. Nevertheless, nephron function, development and cellular specification are highly conserved (Zhou and Vize, 2004; Raciti et al., 2008; Wessely and Tran, 2011). In the present study, we could show that Ctx has a very specific and pronounced effect on proximal tubules. It caused a shortening of the tubular structures by interfering with cell proliferation. At the molecular level, this phenotype was caused by hyperactivation of Gnas signaling via Rapgef4. Moreover, electron microscopy, uptake/secretion studies using a human proximal tubular cell line as well as inhibitors of the exo- and endocytotic pathways suggest that Ctx causes an imbalance of the secretory pathway. As such these experiments demonstrate—for the first time—that vesicular transport is not only important for the functionality of fully differentiated proximal tubules, but is also instrumental for nephron growth.

Materials and methods

Embryo manipulations

Xenopus embryos were obtained by *in vitro* fertilization and maintained in 0.1x modified Barth medium (Sive et al., 2000) and staged according to Nieuwkoop and Faber (1994). Antisense morpholino oligomers were obtained from GeneTools. The sequences of the antisense morpholino oligomers used in this study were 5′-AGA CAC CCC ATG GTC CGT GTG GGC T-3′ (*Gnas-MO*), 5′-CCT AAA CAA CCC ATA TTA ATG GTC C-3′ (*Gnal-MO*) and 5′-CTT GGC GAA ATC CCA TTA CCT CTG T-3′ (*Rapgef4-sMO*). Antisense morpholino oligomers were diluted to a concentration of 1 mM. The *pCS2-Gnas-GFP* and *pCS2-Gnal-GFP* constructs were generated by PCR from *pCMV-SPORT6-Gnas* and *pCMV-SPORT6-Gnal* and subcloned into *pCS2-AcGFP*. For synthetic mRNA all plasmids were linearized with *Not*I and transcribed with SP6 RNA polymerase using the mMessage mMachine® (Ambion). For all the injections a total of 8 nl of morpholino oligomer solution was injected radially at the 2- to 4-cell stage into *Xenopus* embryos. For the GFP reporter assays these injections were followed by two injections of 2 ng synthetic mRNA into two animal blastomeres at the 8-cell stage.

For the drug experiments *Xenopus* embryos were cultured until stage 29/30 and treated with the indicated amounts of the chemical compounds until the untreated controls reached the desired developmental stage. Drugs were replaced every 24 h. With the exception of 6-Bnz-cAMP-AM (cAMP-PKA, Biolog Inc), 8-pCPT-2′-O-Me-cAMP-AM (cAMP-Epac, Biolog Inc), Dynasore (EMD Millipore) and Golgicide A (EMD Millipore) all other compounds were obtained from Sigma.

Xenopus uptake experiments were performed following the paradigm developed by Zhou and Vize (2004). Embryos were exposed to Ctx until stage 35. They were then anesthetized using 500 mg/l MS222 and then injected into the coelomic cavity with approximately 8 nl of Albumin-FITC (1 mg/ml), 10 kD Dextran-FITC (50 μg/ml) or 150 kD Dextran–Rhodamine (50 μg/ml). Three hours later embryos were fixed first in 4% PFA (2 h) followed by Dent's fixative overnight.

Whole mount in situ hybridization

The procedure for the *in situ* hybridizations and the analysis by paraplast sectioning has been previously described (Belo et al., 1997; Tran et al., 2007). To generate antisense probes plasmids were linearized and transcribed as follows: *pSK-Aplnr—Not*I/T7 (Clone ID: 7296250), *pSK-β1-Na/K-ATPase—EcoR*I/T7 (Tran et al., 2007), *pCMV-SPORT6-Gnal—EcoR*I/T7 (Clone ID: 8317937), *pCMV-SPORT6-Gnas—Asp*718/T7 (Clone ID: 6864835), *pSK-Ncc—EcoR*I/T7 (Tran et al., 2007), *pSK-Nkcc2—Sma*I/T7 (Tran et al., 2007), *pCMV-SPORT6-Nphs1*, *Eco*RI/T7 (Tran et al., 2007), *pCMV-SPORT6-Rapgef3—Sal*I/T7 (Clone ID: 5571816), *pSK-Rapgef4—EcoR*I/T7 (Clone ID: XL099e15), *pCMV-SPORT6-Sglt1-K—Sal*I/T7 (Zhou and Vize, 2004), *pCMV-SPORT6-Slc7a7—Sal*I/T7 (Raciti et al., 2008), *pGEM-T-Slc7a13—Sal*I/T7 (Agrawal et al., 2009), *pCMV-SPORT6-Slc25a10—Sal*I/T7 (Raciti et al., 2008).

Histology, immunohistochemistry and proliferation analysis

For histological staining, *Xenopus* embryos were fixed in Bouin's fixative, cleared in 70% ethanol, embedded in paraplast, sectioned at 7 μm, dewaxed, and stained with Hematoxylin and Eosin or Periodic Acid Schiff. For immunohistochemistry embryos were fixed in Dent's fixative (4:1 methanol:DMSO). For whole mount immunostaining, embryos were incubated overnight with the 3G8 and 4A6 monoclonal antibodies (Vize et al., 1995) followed by incubation with a Horseradish peroxidase-coupled anti-mouse secondary antibody and

developed using the ImmPACT DAB kit (Vector Laboratories). The double 3G8/4A6 staining was performed by directly labeling the 4A6 antibody with Zenon® 647 (Invitrogen), while the 3G8 antibody was visualized with anti-mouse Alexa-555. For the analysis of yolk platelet proteins embryos were first processed for 3G8 antibody staining on whole mounts (using anti-mouse Alexa-555 as secondary antibody). Embryos were then embedded in paraplast, sectioned at 25 μm and probed with anti-vitellogenin or anti-seryp antibodies (kind gifts of Dr. M. Kirschner) followed by anti-rabbit Alexa-647. Vitellogenin labeling intensity was quantified by the ImageJ software using only the 3G8-positive tubules of 4–5 sections per embryo and five embryos for each treatment. The proliferation analysis was performed as described previously (Romaker et al., 2012).

Transmission electron microscopy

Embryos were fixed in 2.5% glutaradehyde/4% paraformaldehyde in 0.2 M cacodylate buffer overnight at 4 °C and postfixed in 1% osmium tetroxide for 1 h at 4 °C. After washing in Maleate buffer they were incubated in 1% uranyl acetate for 1 h, washed again and dehydrated into propylene oxide. Samples were infiltrated with Eponate and allowed to polymerize for 24 h. Ultra thin sections of 85 nm were cut with a diamond knife, stained with uranyl acetate and lead citrate, and then observed with a Philips CM12 electron microscope operated at 60 kV.

Uptake and secretion Assays in HK-2 cells

Human proximal tubular cell line, HK-2, was maintained in Ham's F-12/DMEM supplemented with 10% FBS, 1% Pen-Strep (5000 U/ml), 1x ITS (Sigma), 0.7 μg/l Triidothyronine and 60 μg/l epidermal growth factor. Cells were seeded into 6-well plates, grown to confluency and starved overnight. For uptake assays the media was changed to serum-free media containing 50 μg Albumin-FITC (Sigma) in the presence or absence of the indicated amounts of Ctx, cAMP-PKA, cAMP-Epac or Brefeldin-A (BFA). After 24 h cells were washed and the amount of retained Albumin-FITC was measured using a Cytofluor II fluorescence plate reader (PerSeptive Biosystems). Uptake was calculated as the ratio between Albumin-FITC divided by the number of living cells present at the end of the experiment. For secretion assays, cells were exposed to Albumin-FITC for 24 h and the uptake was measured (value M1); cells were then changed to serum-free media without Albumin-FITC, but in the presence or absence of the indicated amounts of Ctx, cAMP-PKA or cAMP-Epac. After another 24 h, cells were washed again and the amount of Albumin-FITC remaining in the cells was measured again (value M2). Secretion was calculated by M1–M2 divided by the number of living cells.

Statistical analysis

All experiments were repeated at least three times using independent fertilizations from different females and the data were analyzed by Student's *t*-test. Dose response curves were generated by non-linear regression using Prism 4 software.

Results

Cholera toxin causes proximal tubule defects

In order to examine the role of GPCRs in *Xenopus* pronephric kidney development, we decided to interfere with the activity of the G-proteins using bacterial toxins (Aktories, 2011). Since we were interested in the later aspects of pronephros development (i.e. size control, specification and terminal differentiation), embryos were treated with the drugs at stage 29/30. At this stage initial specification of the kidney anlage has been completed and the tubules have been patterned along their proximal–distal axis; analysis was performed at

stage 39/40 or later, when the renal epithelial cells are terminally differentiated and the kidney is functional (Vize et al., 2003a; Zhou and Vize, 2004; Reggiani et al., 2007; Raciti et al., 2008; Wessely and Tran, 2011). In the initial experiment embryos were treated with *Pasteurella multocida* toxin (Pmt), Pertussis toxin (Ptx) or Cholera toxin (Ctx) at a dose of 2 μg/ml and morphology and histology were evaluated. Pmt-treated embryos were identical to untreated controls and did not show any overt phenotype (Fig. 1A and B′). Ptx exposure also did not result in any gross morphological effects, but the cells lining the tubules appeared disorganized (Fig. 1C, and C′ and data not shown). It is noteworthy that the dose of Pmt and Ptx used in this study has been shown to be biologically effective (Durieux et al., 1992; Orth et al., 2009) and that even higher concentrations did not cause more pronounced pronephric defects (data not shown). The most dramatic phenotype was observed with Ctx treatment. These embryos developed massive edema caused by fluid accumulation within the embryos (Fig. 1D and D′). Using different concentrations of Ctx, we could establish a dose response curve for edema formation by Ctx with a median effective dose (ED_{50}) of 23 ng/ml (Fig. 1E).

Fluid accumulation in the embryo is one indication of a nonfunctional pronephros, but does not rule out vascular or lymphatic defects (Howland, 1916; Kalin et al., 2009). In fact, it has been previously shown that increasing cAMP levels by Forskolin treatment causes edema by disrupting vascular development (Kalin et al., 2009). Since the primary outcome of Ctx treatment is upregulation of cAMP, we therefore examined the vasculature using *apelin receptor* (*aplnr*) expression as a readout (Devic et al., 1996; Kalin et al., 2009). Whole mount *in situ* hybridization demonstrated that Ctx—like Forskolin—dramatically disrupted vascular gene expression (Fig. 1F and G) suggesting that the edema phenotype was at least in part caused by a vasculature defect.

To examine, whether Ctx also caused defects in the pronephros itself, we used two *Xenopus* kidney-specific antibodies, 3G8 and 4A6. These two antibodies label the proximal tubules or the distal tubules and pronephric duct, respectively ((Vize et al., 1995) and Fig. 1I and K). Upon Ctx treatment the 3G8-positive proximal tubules did not show their normal convolutions, but instead were much smaller and appeared as straight branches only (Fig. 1J). The growth of proximal tubules is highly regulated during pronephros development (D.R and O.W. manuscript in preparation). Indeed, comparing the number of proximal tubular cells between untreated and Ctx-treated embryos demonstrates that there is no difference at stage 35, but proximal tubular expansion is completely blunted at stage 42 in the presence of Ctx (Fig. 1H). Besides this dramatic change in proximal tubular growth, we observed another phenotype when the 4A6 staining was examined. While its pattern in the distal tubules and the pronephric duct was unchanged, Ctx-treated embryos displayed co-labeling with 3G8 and 4A6 the in the proximal tubules (Fig. 1L, indicated by red arrowheads). Like edema formation, ectopic 4A6 staining was concentration-dependent with a nearly identical ED_{50} of 31 ng/ml (Fig. 1E). Since 4A6 has never been reported to label proximal tubules, we co-stained embryos using immunofluorescence by distinguishing the two mouse monoclonal antibodies by Zenon®-labeling (Fig. 1M and N). Paraplast sections of the whole mounts confirmed this observation. Untreated embryos never displayed any co-staining (Fig. 1O and Q), whereas every single section of a 3G8-positive tubule was also labeled with 4A6 in Ctx treated embryos (Fig. 1P and R).

To examine, whether this is due to a change in the patterning of the pronephros along its proximal–distal axis, we performed whole mount *in situ* hybridizations using markers labeling different nephron segments (Zhou and Vize, 2004; Raciti et al., 2008) (Supplementary Fig. S1). The proximal tubular marker *Sglt1K*, as well as *Slc7A7*, *Slc25a10* and *Slc7a13*, markers for the individual proximal tubular sub-domains, were still expressed in Ctx-treated embryos. More importantly, genes labeling the other nephron segments did

not show any ectopic staining in the proximal tubules of Ctx-treated embryos. Based on these data, we conclude that growth of the proximal tubules, but not pronephric patterning and specification is perturbed by Ctx treatment.

Cholera toxin perturbs the cytoarchitecture of proximal tubular cells

The 4A6 antibody recognizes a yet unidentified epitope (Vize et al., 1995). To more thoroughly analyze the phenotype, we examined the ultrastructure of proximal tubules using transmission electron microscopy (TEM) comparing untreated and Ctx-treated embryos at stage 42. Tubules of control embryos were well organized, characterized by cuboidal cell shape, an apical brush border and tight cell–cell junctions (Fig. 2A and A′). In contrast, Ctx-treated proximal tubules were less stereotypical when comparing several specimens. Their cell shape was rather irregular, ranging from cuboidal to more flattened (Fig. 2B and data not shown); cells were also often detached from each other and exhibited large gaps in between (indicated by arrows in Fig. 2B), but they still formed tight junctions (Fig. 2B′ and data not shown). However, the most obvious difference in the TEM between untreated and Ctx-treated samples was the number and size of electron dense black structures, the yolk platelets. These intracellular, membrane bound organelles serve as energy source in amphibians and are gradually used up during embryonic development (Fagotto and Maxfield, 1994; Jorgensen et al., 2009). Untreated embryos exhibited only a few remaining yolk platelets in the proximal tubular cells (Fig. 2A). In contrast, Ctx-treated embryos were markedly enriched in them (Fig. 2B). This conclusion was confirmed in two ways. First, Periodic Acid Schiff (PAS) staining detected many more protein-rich granules in embryos exposed to Ctx (Fig. 2C and D). Secondly, immunofluorescence analysis with an antibody against vitellogenin, the main component of yolk platelets (Jorgensen et al., 2009), demonstrated more vitellogenin-positive yolk platelets in the proximal tubules of Ctx-treated embryos (Fig. 2E and F′). Interestingly, this effect was confined to the proximal tubules, since the distal, 3G8-negative tubules, did not show any differences (indicated by the asterisks in Fig. 2E and F).

To explain the effects of Ctx, we envisioned two possible mechanisms, delayed yolk platelet activation or reduced consumption/degradation. Recently, Jorgensen et al. (2009) showed that the presence of the yolk protein seryp correlates with the activation status of yolk platelets. It is present in inactivated yolk platelets, but is lost when yolk platelets become metabolized. As reported (Jorgensen et al., 2009), seryp expression was detected in the pronephric kidney at stage 35 (data not shown), but not at stage 40 (Fig. 2G). Ctx treatment did not alter this pattern (Fig. 2H and data not shown). This suggested that constitutive active G-protein signaling did not delay activation of yolk platelets, but instead caused reduced vitellogenin consumption/degradation. To directly test the latter hypothesis, we quantified the intensity of the vitellogenin staining in proximal tubules at stage 35 and 40 (Fig. 2I). No effect of Ctx could be detected at the early stage and vitellogenin expression was high under both conditions. At stage 40, yolk platelets were greatly reduced in untreated control embryos. However, Ctx-treated embryos did not show any reduction of staining between the two stages, suggesting that yolk degradation is really impaired. This hypothesis was also supported by the transmission electron microscopy. Besides the electron-dense yolk particles, proximal tubules also exhibit lighter stained structures that are surrounded by a thick membrane layer (Fig. 2A″), which we believe are intermediates of yolk platelet degradation. The same structures were also present in the proximal tubules of Ctx-treated embryos, but were often enclosed by a thinner membranous layer (Fig. 2B″).

Since we have shown that Ctx inhibited proximal tubular cell growth (Fig. 1H), we wanted to distinguish, whether the impaired yolk degradation is a consequence of the absence of proliferation. To this end, we inhibited cell cycle progression using hydroxyurea and aphidicolin (HUA, (Harris and Hartenstein, 1991; Tran et al., 2007)) from stage 29/30

onwards. This caused smaller proximal tubules (data not shown). More importantly, HUA reduced yolk degradation as assayed by vitellogenin staining (Fig. 2J and Supplementary Fig. S2).

Together, these data imply that at the cellular level inhibition of cell growth by Ctx causes accumulation of yolk platelets.

Gnas is the target of cholera toxin

Ctx functions by ribosylating the two members of the $G\alpha_s$ family, Gnas and Gnal, and rendering them constitutively active (Fig. 3A and (Aktories, 2011)). To identify whether the *Xenopus* Ctx phenotype is caused by Gnas, Gnal or a combination of both, we first analyzed the expression of these two G-protein alpha subunits by whole mount *in situ* hybridization. As shown in Fig. 3B *Gnas* mRNA could be detected in the intermediate mesoderm (which includes the pronephric tubules and duct as well as the vasculature), the neural tube and in the brain. On sections *Gnas* was particularly strongly expressed in the proximal tubules with an apical to basolateral gradient (Fig. 3B′ and B″). *Gnal* was localized to the olfactory placode and the nephrostomes of the pronephric kidney (Fig. 3C and C′). Analysis of paraplast sections suggested that there is also low-level expression in pronephric tubules and duct (Fig. 3C″).

Since both G-proteins targeted by Ctx were expressed in the pronephros, either one could be a candidate for the Ctx phenotype. Thus, we next eliminated both of them using antisense morpholino oligomers (MOs) targeting the start codon of either *Gnas* (*Gnas-MO*) or *Gnal* (*Gnal-MO*). The efficacy of the two MOs was verified using GFP fusion proteins (Supplementary Fig. S3). Next, each MO was injected at the 2- to 4-cell stage. Embryos were cultured until stage 29/30 and split into two batches, one of which was treated with 2 μg/ml Ctx, while the other one was kept untreated. At stage 40 embryos were processed for immunohistochemistry with 3G8 and 4A6. As shown above Ctx treatment caused a decrease in proximal tubule size and ectopic 4A6 expression (Fig. 3D, E, K and L). Injection of *Gnal-MO* did not alter the Ctx phenotypes (Fig. 3I and P), suggesting that Gnal is not the target of Ctx in the pronephros. Conversely, injection of *Gnas-MO* rendered embryos insensitive to Ctx. *Gnas-MO* injected embryos exhibited somewhat smaller proximal tubules, but exposure to Ctx did not decrease their size even further (Fig. 3G and J). Similarly, injection of *Gnas-MO* completely abolished ectopic 4A6 staining caused by Ctx treatment (Fig. 3N and Q).

Together these data demonstrate that in the absence of Gnas, Ctx no longer affects the pronephric kidney. This suggests that in the pronephros Ctx functions solely by hyperactivating Gnas, but not Gnal.

Activation of Rapgef4 is responsible for the proximal tubular phenotypes

Canonical downstream signaling of Gnas involves the activation of adenylate cyclase and the generation of cAMP (Fig. 4A and (Weinstein et al., 2007)). Indeed, the adenylate cyclase agonist Forskolin and the phospodiesterase inhibitor IBMX caused identical phenotypes to Ctx (data not shown and (Kalin et al., 2009)). To perform a detailed pathway analysis, embryos were next treated with chemical compounds that either activate or inactivate cAMP signaling (Fig. 4A). Furthermore, to even detect subtle effects experiments were performed using concentrations close to the ED_{50} (30 ng/ml Ctx, 500 ng/ml Forskolin, 150 ng/ml of the PKA-specific cAMP analog 6-Bnz-cAMP-AM (cAMP-PKA) and 100 ng/ml of the Rapgef3/4-specific cAMP analog 8-pCPT-2′-O-Me-cAMP-AM (cAMP-Epac)). As expected, the ED_{50} of Ctx and Forskolin induced the entire range of the phenotype in approximately 50% of the embryos (Fig. 4B F, K, L and S). Surprisingly, when the PKA inhibitor H89 was used, the Ctx phenotype separated into two independent branches. H89

rescued edema formation caused by Ctx or Forskolin, but did not revert the 4A6 and 3G8 staining back to normal (Fig. 4B N and S). The PKA-specific cAMP analog 6-Bnz-cAMP-AM confirmed that edema formation is PKA-dependent (Fig. 4B, O, P and S).

PKA has been regarded as the main target of cAMP, but it has become increasingly clear that there are alternative pathways. Among those Rapgef3/4 (also known as Epac1/2) is the most prominent one (Holz et al., 2006). To examine this, embryos were exposed to 8-pCPT-2′-O-Me-cAMP-AM, a Rapgef3/4-specific cAMP analog. As shown in Fig. 4B and Q–S, this compound showed the opposite result to the one of the PKA agonist. It caused ectopic 4A6/reduced 3G8 staining, but not edema formation.

The conclusion that Ctx signals via Rapgef3/4 was based on the use of a cAMP analog specific for this pathway. Obviously we wanted to complement these experiments with a loss-of-function approach, but a specific Rapgef3/4 antagonist is unavailable (Holz et al., 2006). Therefore, we decided to perform loss-of-function analyses. Since *Rapgef3* mRNA was not detectable in the pronephros, whereas *Rapgef4* was rather ubiquitously expressed with clearly detectable staining in the proximal tubules of the kidney, we focused on Rapgef4 (Fig. 4T and T′ and Supplementary Fig. S4). In the absence of full-length *Xenopus laevis Rapgef4* sequence information we designed an antisense morpholino oligomer that should prevent correct splicing (*Rapgef4-sMO*). Unfortunately, the effects of the *Rapgef4-sMO* were only partial and did not completely abolish correct splicing (Supplementary Fig. S3). But since the aim of the experiment was to rescue the effects of Ctx, we envisioned that even a partial knockdown might suffice. Therefore, *Xenopus* embryos were injected at the 2- to 4-cell stage with *Rapgef4-sMO*, cultured until stage 29/30 and then split into two batches, one kept untreated and the other treated with 2 μg/ml Ctx. At stage 40 embryos were fixed and analyzed by immunohistochemistry with 3G8 and 4A6. Injection of *Rapgef4-sMO* rescued the effect of Ctx treatment (Fig. 4U–BB). Furthermore, and in agreement with the chemical compound analysis *Rapgef4-sMO*-injected embryos did not rescue the edema formation (data not shown).

Based on the data of the pathway analysis, we concluded that there are two independent phenotypes caused by Ctx treatment of *Xenopus* embryos, PKA-dependent edema formation and Rapgef4-dependent defects in proximal tubular development. Since edema formation by Ctx is likely due to impaired vasculogenesis (Fig. 1G), activation of PKA should also interfere with vasculogenesis. To test this, we performed whole mount *in situ* hybridization with *aplnr* on embryos treated with the different agonists/antagonists. As shown in the Supplementary Fig. S5 this was indeed the case. PKA-dependent signaling was responsible for disruption of *aplnr* expression, whereas activation of Rapgef4 by 8-pCPT-2′-O-Me-cAMP-AM did not cause any changes.

Together, these data indicate that in the developing *Xenopus* embryo Ctx regulates vasculogenesis by activating PKA and proximal tubular growth by activating Rapgef4.

Rapgef3/4 signaling regulates uptake and secretion in proximal tubular cells

Rapgef4 regulates endo- and exocytosis in a variety of settings (Shibasaki et al., 2007; Lee et al., 2012). Thus, we wondered, whether the proximal tubular phenotypes were cause by a defect in endo- or exocytosis. To this end, we examined protein uptake in the *Xenopus* tubules as previously described (Zhou and Vize, 2004). Untreated as well as Ctx treated embryos were injected with Albumin-FITC into the coelomic cavity. Embryos were fixed after three hours and processed for 3G8 staining to visualize the proximal tubules. Consistent with the high expression of endocytic receptors in proximal tubules (Christensen et al., 2008), Albumin was primarily taken up in the proximal tubules both in untreated as well as Ctx-treated embryos (Fig. 5A and B‴). Identical results were obtained using 10 kD

Dextran-FITC and 150 kD Dextran–Rhodamine (Supplementary Fig. S6). However, when comparing paraplast sections of the whole mounts it appeared that Ctx resulted in an increased Albumin-FITC uptake (Fig. 5A‴ and B‴). Unfortunately, the experimental paradigm was too variable to exactly quantify the precise level of protein uptake.

To obtain accurate measurements, we decided to utilize the human proximal tubular cell line, HK-2. These cells express the two required apical transport receptors megalin and cubulin and are well established for uptake studies (Li et al., 2008; Basnayake et al., 2010). To quantify how Ctx signaling affects protein uptake, confluent cells were starved for 24 h, exposed to Albumin-FITC in the absence or presence of Ctx, cAMP-PKA, cAMP-Epac or BFA for an additional 24 h and then measured (Fig. 5C). Different concentrations of Ctx (0.1, 1, 10 μg/ml) increased the uptake of Albumin-FITC in a dose dependent manner (Fig. 5D and Supplementary Fig. S6). This effect was Rapgef3/4-dependent as only cAMP-Epac but not cAMP-PKA could mimic the consequence of Ctx treatment. Moreover, the Rapgef3/4 antagonist BFA showed the opposite result and decreased uptake in a concentration-dependent manner. Since endo- and exocytosis are often linked, we next tested whether Ctx also affects protein secretion. We followed a similar paradigm as before, but this time allowed cells to take up Albumin-FITC in the absence of chemical compounds and then analyzed its secretion in the presence of drugs (Fig. 5E). In fact, Rapgef3/4 signaling also regulated dose-dependent secretion of Albumin-FITC (Fig. 5F).

Together these data show that Ctx can effectively modulate the secretory behavior of proximal tubular cells by increasing uptake and decreasing secretion.

Imbalance of endo- and exocytosis by Ctx causes proximal tubular defects

Proliferation is triggered by the secretion of a growth factor, its binding to a cell surface receptor, the activation of a downstream signaling pathway and the endocytosis of the receptor to subsequently terminate the signal. As such, the growth inhibition observed in the proximal tubules of the Ctx-treated *Xenopus* embryos, may be explained by the defects in endo- and exocytosis observed in the proximal tubular cell line upon exposure to Ctx. To test this hypothesis we treated embryos with the endocytosis inhibitor Dynasore and Golgicide A, a GBF1 inhibitor, which arrests secretion of soluble and membrane-associated proteins (Macia et al., 2006; Saenz et al., 2009).

Since Ctx increases endocytosis in HK-2 cells, we tested whether addition of Dynasore rescued Ctx-treated embryos. Embryos treated with 50 mM Dynasore alone exhibited smaller proximal tubules (Fig. 6A, E and K). However, when combined with Ctx (using its EC_{50} dose), the cell numbers resembled those of Dynasore and not those of Ctx (Fig. 6C, E, G and K). This suggested that proximal tubular growth defect caused by Ctx was at least in part due to the increased endocytosis. In contrast, the ectopic 4A6 staining was mostly independent of endocytosis. Dynasore alone caused some ectopic 4A6 staining, but could not significantly rescue the effects of Ctx treatment (Fig. 6B, D, F, H and L).

In HK-2 cells Ctx decreased exocytosis. If this was also relevant in *Xenopus* embryos, interfering with of exocytosis by Golgicide A should induce a similar phenotype as Ctx. Indeed, addition of Golgicide A reduced the size of the proximal tubules and caused ectopic 4A6 staining (Fig. 6I, J, M and N).

Together these data suggests that in the frog regulation of endo- and exocytosis by Ctx are also responsible for the proximal tubular defects.

Discussion

Xenopus is a powerful system to study signaling pathways using low molecular weight compounds that are simply added to the culture medium (Adams and Levin, 2006). Here we used such an approach to study the function of G-proteins during later aspects of pronephros development. Using three toxins, Pmt, Ptx and Ctx, we grossly perturbed G-protein signaling. Interestingly, only Pmt did not show any obvious phenotype in kidney formation or function. Ptx treatment caused cell shape changes in the pronephric kidney characterized by thicker cell diameters as well as disruption of the simple cuboidal epithelium (data not shown). This suggests a defect in cell behavior and one potential signaling pathway affected by Ptx is non-canonical Wnt signaling. This pathway involves G-proteins and, indeed, Ptx has been shown to perturb Wnt activity during tissue separation of the *Xenopus* gastrula (Winklbauer et al., 2001; Katanaev et al., 2005; Angers and Moon, 2009). Furthermore, several components of the non-canonical Wnt signaling pathway are expressed in the developing *Xenopus* pronephros (Zhang et al., 2011) and Frizzled-8 has been implicated in the morphogenetic processes regulating proximal tubular growth (Satow et al., 2004; Lienkamp et al., 2010).

The toxin causing the most prominent defects was Ctx. It specifically interferes with two G-proteins, Gnas and Gnal. While we did not identify a contribution of Gnal to the Ctx phenotype, tight regulation of Gnas activity is clearly very important during late stages of *Xenopus* embryonic development. Hyperactivation of Gnas results in severe defects in at least two different organs, the vasculature and the pronephros. During vascular development, it has previously been shown that an increase in cAMP levels interferes with blood vessel development (Kalin et al., 2009). This study confirmed those results and extended them by demonstrating that this phenotype is due to the activation of PKA.

In the pronephros, Ctx caused a reduction of proximal tubules, ectopic expression of 4A6 and delayed processing of yolk platelets. In particular, the impairment of proximal tubular growth was very striking. While tubules normally increase in size during development (Fig. 1H and D.R and O.W. manuscript in preparation), Ctx completely inhibited this process. We believe that this phenotype is due to an imbalance of endo- and exocytosis (Fig. 6O). Ctx activates Rapgef4, which in turn increases endocytosis and decreases exocytosis. Based on the epistasis experiments with Dynasore and Golgicide A we favor the following scenario: (1) the proximal tubules secrete a growth factor that is required for cell growth (exocytosis); (2) this (or any other) growth factor binds to its receptor and activates signaling; (3) the ligand receptor complex becomes internalized to terminate the signal (endocytosis). Upon treatment with Ctx this signaling cascade is disrupted at the level of ligand secretion (which is impaired) and receptor internalization (which is accelerated). The net effect of these changes can easily explain the growth defects observed. Obviously, it will be very important to identify the nature of this signal in the future and test how it is affected by Ctx.

This hypothesis also explains why Ctx resulted in a dramatic increase of vitellogenin-positive yolk platelets in the proximal, but not the distal tubules (Fig. 2). It has recently been proposed that yolk degradation is initiated by nutritional needs (Jorgensen et al., 2009). Since Ctx directly interferes with the proliferation of proximal tubular cells, this obviously reduces the energy need of those cells. As a consequence yolk degradation is decreased and yolk platelets are retained.

Finally, a defect in endosomal transportation also explains another very surprising observation, the fact that proximal tubular cells stain positive with the 4A6 antibody. In the *Xenopus* field, the two antibodies 3G8 and 4A6 have been extensively used to examine pronephros development. Yet, this—to our knowledge—is the first demonstration that

proximal tubular cells co-stain for both antibodies. This was not due to delayed differentiation, since ectopic 4A6 staining persisted until at least stage 42 (data not shown); nor was it due to transdifferentiation of proximal tubules, since the proximal tubules did not acquire the expression of genes characteristic for intermediate or distal tubules nor did they lose staining for any proximal tubular marker genes. Unfortunately, the nature of this co-staining remains unclear, because both antibodies recognize unknown epitopes. We currently favor the hypothesis that 4A6 recognizes a secreted protein that is present in all cells of the pronephros. However, proximal tubules have such a high secretion rate compared to the remainder of the pronephros that 4A6 is normally undetectable in these cells. Ctx treatment would alter proximal tubular cells so that their secretory function is less effective and causes the accumulation of the 4A6 protein. This explanation is in line with the data that inhibition of endocytosis has little effect on ectopic 4A6 staining, whereas inhibition of secretion is sufficient to cause it. Obviously confirmation of this hypothesis requires the identification of the protein recognized by the 4A6 antibody.

One of the main conclusions of the study is that G-protein activity needs to be tightly controlled during pronephros development and too much cAMP is detrimental. Interestingly, the opposite is not true and too little cAMP has rather subtle consequences. Inhibiting PKA by H89 did not result in any pronephric defects. In hindsight, this is not too surprising, since cAMP/PKA regulates water homeostasis in the metanephric kidney and the main defect of too little cAMP is dehydration. However, *Xenopus* embryos live in an aqueous environment and are hypertonic. Therefore they passively take up water constantly and lowering cAMP should have little effect. This is underscored by the observation that the pronephric kidney lacks one of the main targets of cAMP/PKA in the metanephric kidney, the cystic fibrosis transmembrane conductance regulator (CFTR) (data not shown).

In respect to Rapgef4 signaling we indeed did observe a subtle loss-of-function phenotype. Loss-of-Rapgef4 (as well as Gnas) caused reduced 4A6 (Fig. 4V and Z and Fig. 3M and N), which is the opposite of ectopic 4A6 staining caused by gain-of-function. However, the phenotype was still much more moderate than using the Rapgef3/4 antagonist Brefeldin-A (data not shown). This could be due to the fact that the *Rapgef4-MO* does not completely inhibit the gene (Supplementary Fig. S3) or is compensated by Rapgef3. Consistent with this, mouse mutants of Rapgef4 have much subtler phenotypes than the Rapgef3/4 double mutants (Shibasaki et al., 2007; Yang et al., 2012).

In conclusion, the present study makes a strong statement for the importance of G-protein signaling on pronephric kidney development. This study focused on downstream effectors, but one obvious question is their upstream regulation by GPCRs. While several GPCRs that cause activation of PKA via Gnas have been identified (e.g. Vasopressin receptor or PTH receptor), the same is not true for Rapgef4. In the future, one will need to examine individual GPCRs and identify those that actually signal to Rapgef4. This will not only result in a better understanding of G-proteins in the pronephric kidney, but also for more general aspects of kidney function and even human diseases caused by mutations in Gnas.

Supplementary Material

Refer to Web version on PubMed Central for supplementary material.

Acknowledgments

We would like to thank Dr. T. Obara and all laboratory members for critically reviewing the manuscript and helpful discussions. *pSK-Rapgef4* was provided by the RIKEN BRC through the National Bio-Resource Project of the MEXT, Japan; the 3G8 and 4A6 antibodies were a kind gift of Dr. E. Jones. The 150 kD Dextran used in this work was made available through a grant (3R01DK078209-04S1) to Dr. Tomoko Obara, OUHSC, Oklahoma. D.R. was

supported by a postdoctoral fellowship from the DFG (RO4124/1-1). This work was supported by a grant from NIH/NIDDK (5R01DK080745-04) to O.W.

References

Adams DS, Levin M. Inverse drug screens: a rapid and inexpensive method for implicating molecular targets. Genesis. 2006; 44:530–540. [PubMed: 17078061]

Agrawal R, Tran U, Wessely O. The miR-30 miRNA family regulates Xenopus pronephros development and targets the transcription factor Xlim1/Lhx1. Development. 2009; 136:3927–3936. [PubMed: 19906860]

Aktories K. Bacterial protein toxins that modify host regulatory GTPases. Nat Rev Microbiol. 2011; 9:487–498. [PubMed: 21677684]

Angers S, Moon RT. Proximal events in Wnt signal transduction. Nat Rev Mol Cell Biol. 2009; 10:468–477. [PubMed: 19536106]

Basnayake K, Ying WZ, Wang PX, Sanders PW. Immunoglobulin light chains activate tubular epithelial cells through redox signaling. J Am Soc Nephrol. 2010; 21:1165–1173. [PubMed: 20558542]

Belo JA, Bouwmeester T, Leyns L, Kertesz N, Gallo M, Follettie M, De Robertis EM. *Cerberus-like* is a secreted factor with neutralizing activity expressed in the anterior primitive endoderm of the mouse gastrula. Mech Dev. 1997; 68:45–57. [PubMed: 9431803]

Borland G, Smith BO, Yarwood SJ. EPAC proteins transduce diverse cellular actions of cAMP. Br J Pharmacol. 2009; 158:70–86. [PubMed: 19210747]

Christensen EI, Raciti D, Reggiani L, Verroust PJ, Brandli AW. Gene expression analysis defines the proximal tubule as the compartment for endocytic receptor-mediated uptake in the Xenopus pronephric kidney. Pflugers Arch. 2008; 456:1163–1176. [PubMed: 18551302]

Devic E, Paquereau L, Vernier P, Knibiehler B, Audigier Y. Expression of a new G protein-coupled receptor X-msr is associated with an endothelial lineage in Xenopus laevis. Mech Dev. 1996; 59:129–140. [PubMed: 8951791]

Durieux ME, Salafranca MN, Lynch KR, Moorman JR. Lysophosphatidic acid induces a pertussis toxin-sensitive Ca(2+)-activated Cl− current in *Xenopus laevis* oocytes. Am J Physiol. 1992; 263:C896–C900. [PubMed: 1415674]

Fagotto F, Maxfield FR. Changes in yolk platelet pH during Xenopus laevis development correlate with yolk utilization. A quantitative confocal microscopy study. J Cell Sci. 1994; 107 (Pt 12): 3325–3337. [PubMed: 7706389]

Harris WA, Hartenstein V. Neuronal determination without cell division in Xenopus embryos. Neuron. 1991; 6:499–515. [PubMed: 1901716]

Heisenberg CP, Solnica-Krezel L. Back and forth between cell fate specification and movement during vertebrate gastrulation. Curr Opin Genet Dev. 2008; 18:311–316. [PubMed: 18721878]

Holz GG, Kang G, Harbeck M, Roe MW, Chepurny OG. Cell physiology of cAMP sensor Epac. J Physiol. 2006; 577:5–15. [PubMed: 16973695]

Howland RB. On the effect of removal of the pronephros of the amphibian embryo. Proc Natl Acad Sci USA. 1916; 2:231–234. [PubMed: 16586615]

Jorgensen P, Steen JA, Steen H, Kirschner MW. The mechanism and pattern of yolk consumption provide insight into embryonic nutrition in Xenopus. Development. 2009; 136:1539–1548. [PubMed: 19363155]

Kalin RE, Banziger-Tobler NE, Detmar M, Brandli AW. An *in vivo* chemical library screen in Xenopus tadpoles reveals novel pathways involved in angiogenesis and lymphangiogenesis. Blood. 2009; 114:1110–1122. [PubMed: 19478043]

Katanaev VL, Ponzielli R, Semeriva M, Tomlinson A. Trimeric G protein-dependent frizzled signaling in Drosophila. Cell. 2005; 120:111–122. [PubMed: 15652486]

Katritch V, Cherezov V, Stevens RC. Diversity and modularity of G protein-coupled receptor structures. Trends Pharmacol Sci. 2012; 33:17–27. [PubMed: 22032986]

Lee YJ, Kim MO, Ryu JM, Han HJ. Regulation of SGLT expression and localization through Epac/PKA-dependent caveolin-1 and F-actin activation in renal proximal tubule cells. Biochim Biophys Acta. 2012; 1823:971–982. [PubMed: 22230192]

Li M, Balamuthusamy S, Simon EE, Batuman V. Silencing megalin and cubilin genes inhibits myeloma light chain endocytosis and ameliorates toxicity in human renal proximal tubule epithelial cells. AJP Renal Physiol. 2008; 295:F82–F90.

Lienkamp S, Ganner A, Boehlke C, Schmidt T, Arnold SJ, Schafer T, Romaker D, Schuler J, Hoff S, Powelske C, Eifler A, Kronig C, Bullerkotte A, Nitschke R, Kuehn EW, Kim E, Burkhardt H, Brox T, Ronneberger O, Gloy J, Walz G. Inversin relays Frizzled-8 signals to promote proximal pronephros development. Proc Natl Acad Sci USA. 2010; 107:20388–20393. [PubMed: 21059920]

Macia E, Ehrlich M, Massol R, Boucrot E, Brunner C, Kirchhausen T. Dynasore, a cell-permeable inhibitor of dynamin. Dev Cell. 2006; 10:839–850. [PubMed: 16740485]

Nieuwkoop, PD.; Faber, J. Normal Table of *Xenopus laevis*. Garland Publishing, Inc; New York: 1994.

Orth JH, Preuss I, Fester I, Schlosser A, Wilson BA, Aktories K. Pasteurella multocida toxin activation of heterotrimeric G proteins by deamidation. Proc Natl Acad Sci USA. 2009; 106:7179–7184. [PubMed: 19369209]

Raciti D, Reggiani L, Geffers L, Jiang Q, Bacchion F, Subrizi AE, Clements D, Tindal C, Davidson DR, Kaissling B, Brandli AW. Organization of the pronephric kidney revealed by large-scale gene expression mapping. Genome Biol. 2008; 9:R84. [PubMed: 18492243]

Reggiani L, Raciti D, Airik R, Kispert A, Brandli AW. The prepattern transcription factor Irx3 directs nephron segment identity. Genes Dev. 2007; 21:2358–2370. [PubMed: 17875669]

Romaker D, Zhang B, Wessely O. An immunofluorescence method to analyze the proliferation status of individual nephron segments in the Xenopus pronephric kidney. Methods Mol Biol. 2012; 886:121–132. [PubMed: 22639256]

Saenz JB, Sun WJ, Chang JW, Li J, Bursulaya B, Gray NS, Haslam DB. Golgicide A reveals essential roles for GBF1 in Golgi assembly and function. Nat Chem Biol. 2009; 5:157–165. [PubMed: 19182783]

Satow R, Chan TC, Asashima M. The role of Xenopus frizzled-8 in pronephric development. Biochem Biophys Res Commun. 2004; 321:487–494. [PubMed: 15358202]

Saxén, L. Organogenesis of the Kidney. Cambridge University Press; Cambridge, UK: 1987.

Shibasaki T, Takahashi H, Miki T, Sunaga Y, Matsumura K, Yamanaka M, Zhang C, Tamamoto A, Satoh T, Miyazaki J, Seino S. Essential role of Epac2/Rap1 signaling in regulation of insulin granule dynamics by cAMP. Proc Natl Acad Sci USA. 2007; 104:19333–19338. [PubMed: 18040047]

Sive, HL.; Grainger, RM.; Harland, RM. Early Development of Xenopus Laevis: A Laboratory Manual. Cold Spring Harbor Laboratory Press; Cold Spring Harbor, New York: 2000.

Smith, HW. From Fish to Philosopher. Little, Brown; Boston: 1953.

Tran U, Pickney LM, Ozpolat BD, Wessely O. Xenopus bicaudal-C is required for the differentiation of the amphibian pronephros. Dev Biol. 2007; 307:152–164. [PubMed: 17521625]

Vize, PD.; Carroll, TJ.; Wallingford, JB. Induction, development, and physiology of the pronephric tubules. In: Vize, PD.; Woolf, AS.; Bard, JBL., editors. The Kidney: From Normal Development to Congenital Disease. Academic Press; Amsterdam: 2003a. p. 19-50.

Vize PD, Jones EA, Pfister R. Development of the Xenopus pronephric system. Dev Biol. 1995; 171:531–540. [PubMed: 7556934]

Vize, PD.; Woolf, A.; Bard, J. The Kidney: From Normal Development to Congenital Diseases. Academic Press; Amsterdam: 2003b.

Weinstein LS, Xie T, Zhang QH, Chen M. Studies of the regulation and function of the Gs alpha gene Gnas using gene targeting technology. Pharmacol Ther. 2007; 115:271–291. [PubMed: 17588669]

Wessely O, Tran U. Xenopus pronephros development-past, present, and future. Pediatr Nephrol. 2011; 26:1545–1551. [PubMed: 21499947]

Winklbauer R, Medina A, Swain RK, Steinbeisser H. Frizzled-7 signalling controls tissue separation during Xenopus gastrulation. Nature. 2001; 413:856–860. [PubMed: 11677610]

Yang Y, Shu X, Liu D, Shang Y, Wu Y, Pei L, Xu X, Tian Q, Zhang J, Qian K, Wang YX, Petralia RS, Tu W, Zhu LQ, Wang JZ, Lu Y. EPAC null mutation impairs learning and social interactions via aberrant regulation of miR-124 and Zif268 translation. Neuron. 2012; 73:774–788. [PubMed: 22365550]

Zhang B, Tran U, Wessely O. Expression of Wnt signaling components during Xenopus pronephros development. PloS One. 2011; 6:e26533. [PubMed: 22028899]

Zhou X, Vize PD. Proximo-distal specialization of epithelial transport processes within the Xenopus pronephric kidney tubules. Dev Biol. 2004; 271:322–338. [PubMed: 15223337]

Appendix A. Supporting information

Supplementary data associated with this article can be found in the online version at http://dx.doi.org/10.1016/j.ydbio.2013.01.017.

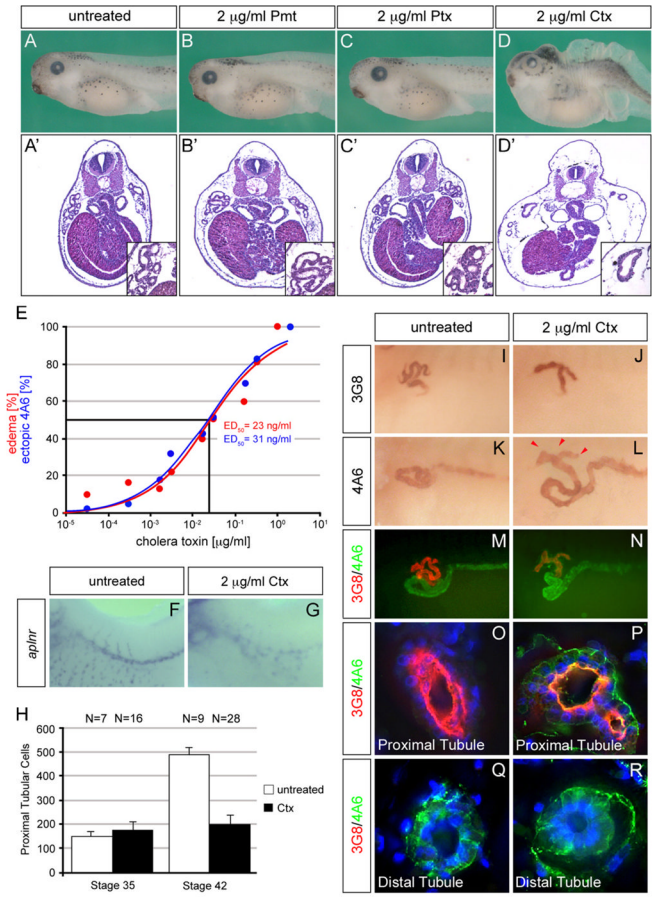

Fig. 1.

Cholera toxin causes proximal tubule defects. (A–D′) *Xenopus* embryos were treated with *Pasteurella multocida* toxin (Pmt), Pertussis toxin (Ptx) or Cholera toxin (Ctx) from stage 29/30 until stage 42 and analyzed by morphology (A–D) and H&E staining (A′–D′). Note that only Ctx causes edema formation. (E) Dose response curves for edema formation (red) and ectopic 4A6 staining (blue) of embryos treated with different doses of Ctx. Each individual data point is the summary of three independent experiments. The curve was obtained by fitting the data using non-linear regression and used to calculate the median effective doses (ED_{50}). (F and G) Whole mount *in situ* hybridization with *aplnr* comparing untreated and Ctx treated embryos at stage 39. (H) Bar diagram depicting the number of proximal tubular cells at stage 35 and 42 in untreated and Ctx treated embryos. (I–R) Ctx-treated embryos were analyzed using the 3G8 and 4A6 antibodies at stage 40 in whole mounts (I–N) or paraplast sections thereof (O–R). Single immunostainings were visualized with DAB, while double stainings were carried out using fluorescent labeled secondary antibodies visualizing 3G8 in red and 4A6 in green. Nuclei were counterstained using DAPI (blue). Ectopic 4A6 staining is indicated by red arrowheads (L).

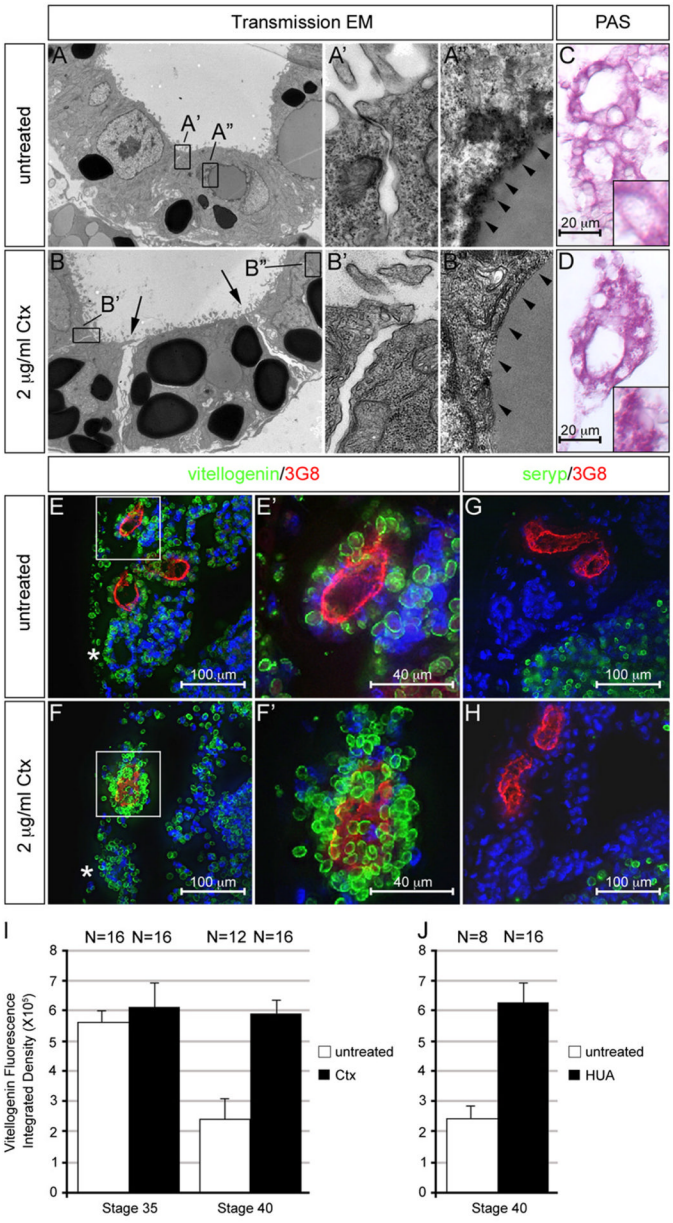

Fig. 2.

Interfering with proximal tubular growth caused a defect in yolk platelet degradation. (A to B″) *Xenopus* embryos were treated with 2 μg/ml Ctx at stage 29/30 and analyzed at stage 42 using transmission electron microscopy at a 2650-fold (A and B) or 31,000-fold magnification (A′, A″, B′ and B″). Position of the insets is indicated by the black boxes in (A and B). Arrows indicate the gaps between the proximal tubular cells upon Ctx treatment, arrowheads point towards the membrane layer surrounding the degrading yolk platelets. (C and D) PAS staining to visualize protein-rich granules in the proximal tubules. Inset shows close-up of a single cell. (E and H) Immunofluorescence staining of proximal tubules using 3G8 (red), anti-vitellogenin or anti-seryp antibodies (green). (E′ and F′) are close-ups of the proximal tubules indicated by white boxes in (E and F); the asterisks indicate the distal tubules; nuclei were counterstained with DAPI (blue). (I and J) Quantification of anti-

vitellogenin staining for untreated and Ctx treated embryos at stage 35 and 40 (I) as well as untreated and treated with Hydroxyurea/Aphidicolin (HUA) at stage 40 (J).

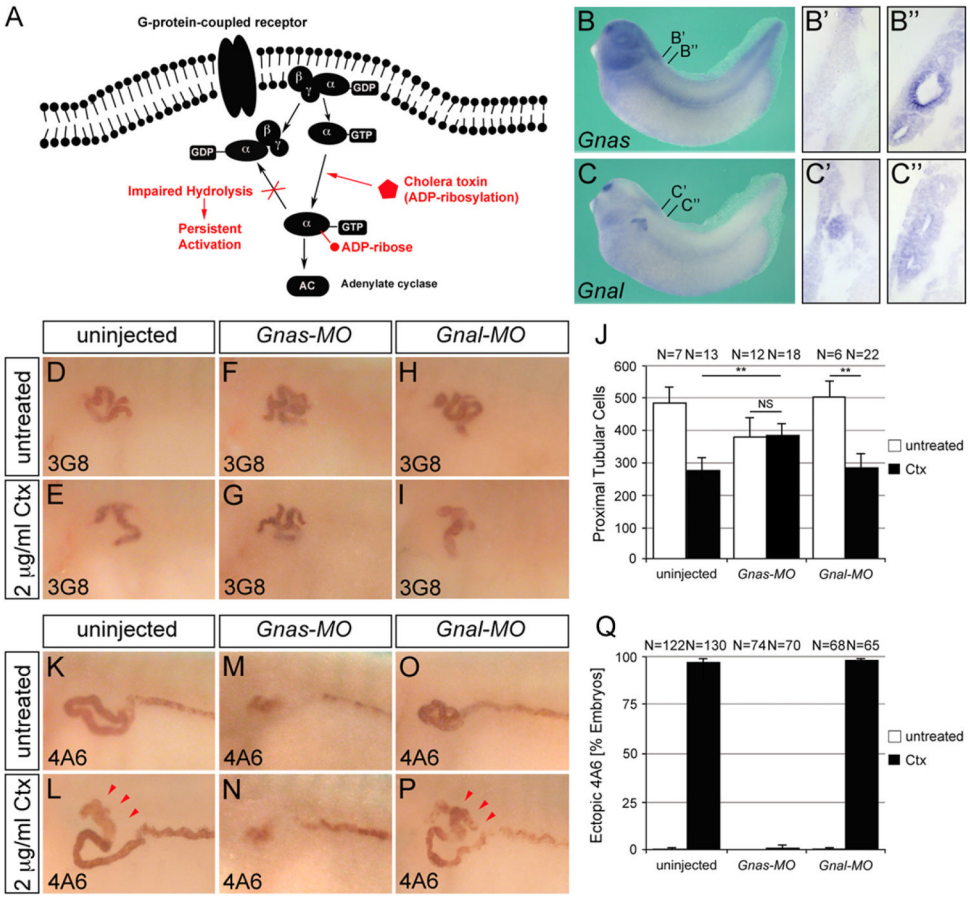

Fig. 3.

Gnas is the target of cholera toxin action. (A) Schematic of signaling via the $G\alpha_s$ G-protein family. The activity of Ctx is indicated in red. (B and C‴) *In situ* hybridization of *Xenopus* embryos at stage 35 for *Gnas* and *Gnal* mRNA by whole mount or paraplast sections thereof. The position of the transverse sections is indicated in (B and C). (D–Q) Whole mount immunostaining with the 3G8 (D–I) and 4A6 antibody (K–P) in control embryos or embryos injected with the *Gnas-MO* or the *Gnal-MO* in the presence or absence of 2 µg/ml Ctx at stage 40. Ectopic 4A6 staining is indicated by red arrowheads. Quantification of proximal tubular cell numbers at stage 42 (J) and ectopic 4A6 staining at stage 40 (Q) summarizing three independent experiments. Data were analyzed by Student's *t*-test with indicating a *p* value of <0.01.

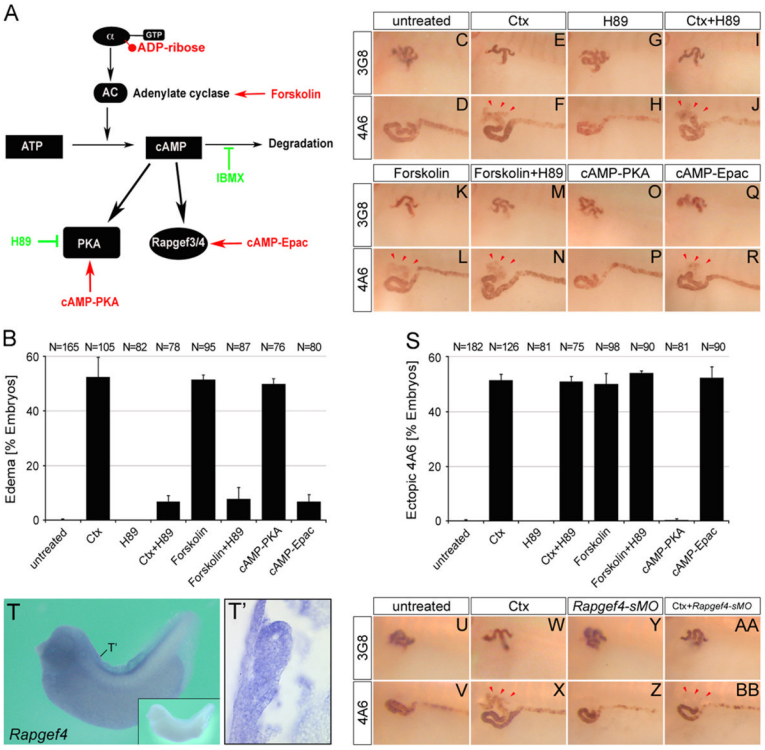

Fig. 4.

Activation of Rapgef4 is responsible for the proximal tubular phenotypes. (A) Schematic diagram depicting how Gnas signals to PKA and Rapgef3/4. Pathway agonists and antagonists are indicated in red or green, respectively. (B–S) *Xenopus* embryos were treated with multiple compounds modulating Gnas signaling and analyzed for edema formation at stage 42 (B) and 3G8/4A6 staining (C–S). Red arrowheads indicate ectopic 4A6 staining. Note that all the agonists were used at an ED_{50} concentration to provide a more sensitive experimental setup. (T and T') *In situ* hybridization of *Xenopus* embryos at stage 35 for *Rapgef4* mRNA by whole mount or paraplast sections thereof. The position of the transverse section is indicated in (T). Close-up in (T) shows the sense control. (U–BB) Whole mount immunostaining with the 3G8 and 4A6 antibody of control embryos or embryos injected with the *Rapgef4-sMO* in the presence or absence of 2 μg/ml Ctx at stage 40. Ectopic 4A6 staining is indicated by red arrowheads in (X) and (BB).

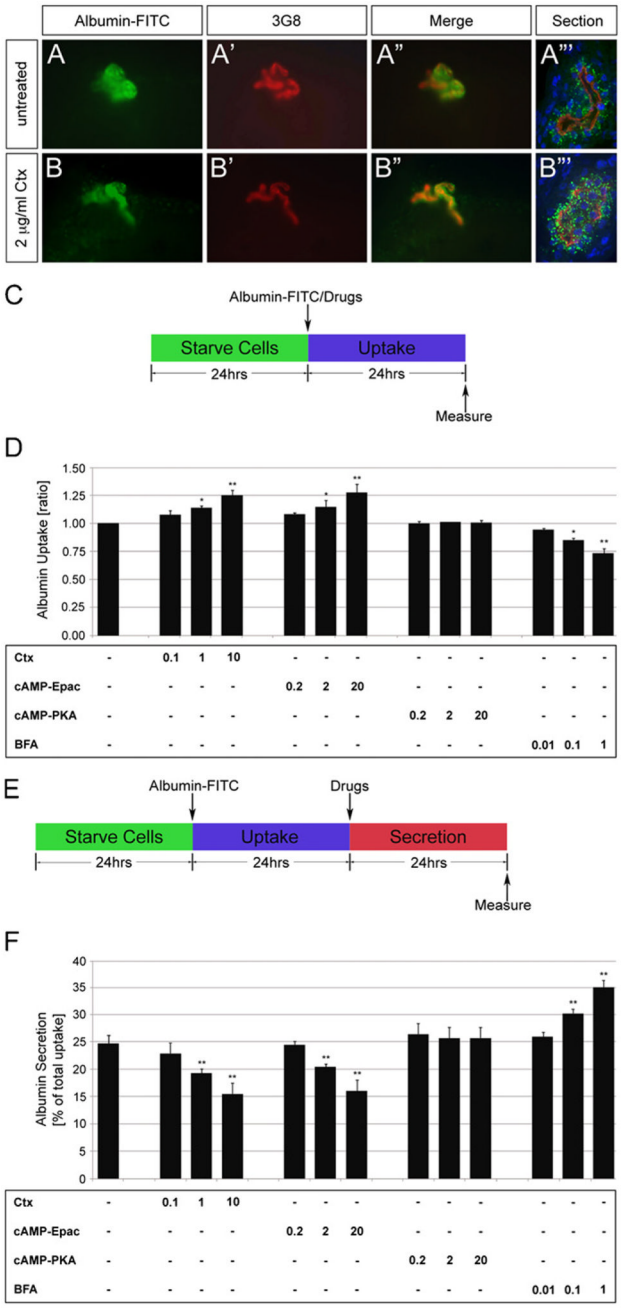

Fig. 5.

Cholera toxin regulates albumin uptake and secretion. (A–B‴) Untreated or Ctx-treated *Xenopus* embryos were injected with Albumin-FITC (green) at stage 35. Embryos were fixed after 3 h, stained with 3G8 (red) and examined in whole mounts (A and A″, B and B″) and sections thereof (A‴ and B‴). DAPI was used to counterstain nuclei (blue). (C) Schematic for the uptake assay in HK-2 cells. (D) Bar diagram of Albumin-FITC uptake of HK-2 cells treated with different doses of Ctx, cAMP-Epac, cAMP-PKA and BFA. (E) Schematic for the secretion assay in HK-2 cells. (F) Bar diagram of Albumin-FITC secretion of HK-2 cells treated with different doses of Ctx, cAMP-Epac, cAMP-PKA and BFA. Data were analyzed by Student's *t*-test with indicating a p value of <0.05 and a p value of <0.01.

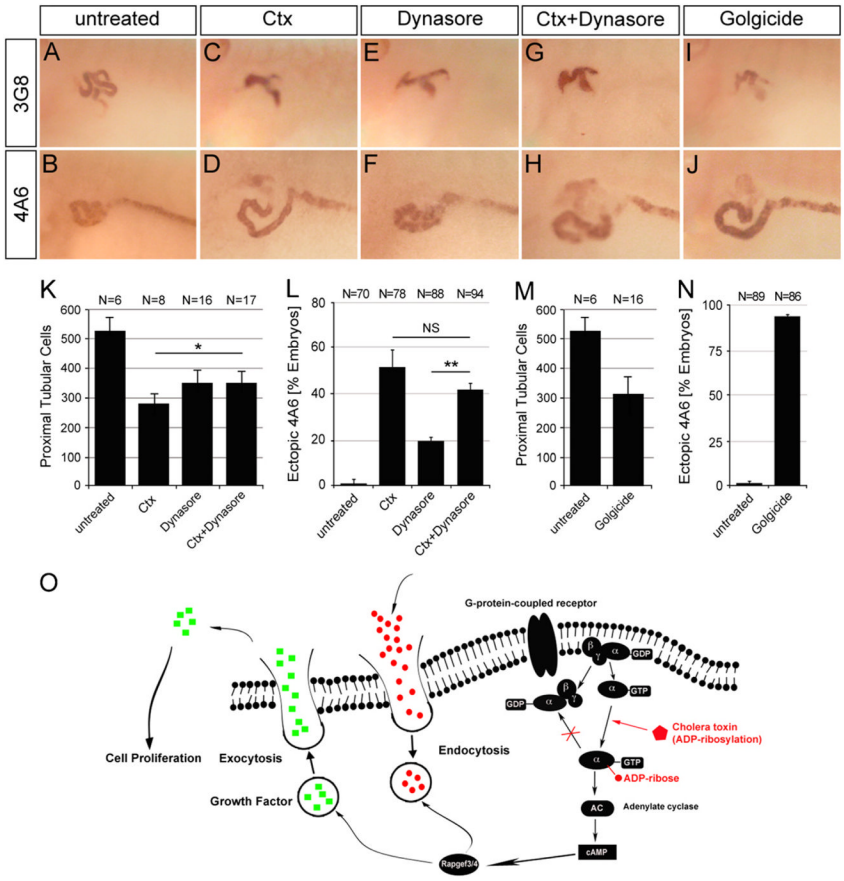

Fig. 6.

Imbalance of endo- and exocytosis by Ctx causes proximal tubular defects. (A–J) Whole mount immunostaining with the 3G8 and 4A6 antibody of control embryos or embryos treated with 50 mM Dynasore in the presence or absence of 2 μg/ml Ctx or 50 μM Golgicide A at stage 40. (K–N) Bar diagrams quantifying proximal tubular cell numbers at stage 42 (K and M) and ectopic 4A6 staining at stage 40 (L and N) summarizing three independent experiments. Data were analyzed by Student's *t*-test with indicating a *p* value of <0.05 and a *p* value of <0.01. (O) Schematic diagram depicting the proposed mechanism of Ctx in *Xenopus* embryos (see text for details).